RSC Advances

PAPER

View Article Online
View Journal | View Issue

Cite this: *RSC Adv.*, 2026, **16**, 3121

Reinforced lignin-based polyurethane foams with improved heat-insulating performance by using cellulose fibers

Chuanyuan Yang,[a] Guoyu Tian,[a] Changjian Wang,[b] Bao Wang,[c] Yuquan Zhang,[c] Zhulin Li,[a] Jingshun Zhuang,[d] Chuanmin Geng*[a] and Zhaojiang Wang *[a]

The incorporation of natural polymers into the synthesis of functional materials such as polyurethanes provides an effective approach for value-added biomass utilization. In this study, Lignin-containing polyol (LP) was prepared by simply mixing Kraft lignin, polyethylene glycol, and glycerol at mass ratio of 3 : 3.5 : 0.5. Lignin-based polyurethane foam (LPUF) was then prepared by mixing LP and polymethylene diphenyl diisocyanate (PMDI) using water as a foaming agent. Cellulose fibers from wood at various loadings (0%, 0.2%, 0.5%, 0.7%, and 1.0%) were incorporated as reinforcing skeletons to investigate the effects on the mechanical properties of LPUF. The results showed that the compressive strength, the flexural strength, and the tensile strength of LPUF were significantly increased by 72.3%, 154.5%, and 244.1% by 0.5% cellulose fiber addition, and reached 647.6 kPa, 1.28 MPa, and 1.17 MPa, respectively. Furthermore, improvement of thermal insulation performance of LPUF was also observed by the decrease of thermal conductivity from 0.0413 W m^{-1} K^{-1} to 0.0378 W m^{-1} K^{-1} by 0.5% cellulose fiber addition. However, cellulose fiber addition over 0.5% resulted in irregular pore morphology, ultimately impairing the mechanical performance of the LPUF. Cellulose and lignin are the major constructional constituents of woody biomass. The application of these natural polymers in polyurethane materials contributes to sustainable development and carbon neutrality.

Received 9th December 2025
Accepted 20th December 2025

DOI: 10.1039/d5ra09512c

rsc.li/rsc-advances

1 Introduction

Polyurethane (PU) is a polymer containing characteristic urethane groups, which exhibits flexibility, elasticity, shape memory, insulation, and the ability to impart structural rigidity to components.[1] PU accounts for about 8% of the total global plastic consumption.[2] Because the properties of PU can be tailored by adjusting the type and proportions of its components, PU has been widely used in thermoplastic plastics, foams, elastomers, adhesives, coatings, and sealants.[3,4]

Among various polyurethane materials, LPUF is particularly notable for its excellent thermal insulation performance.[5,6] It has been widely applied in pipeline insulation, building insulation, cushioning, and food refrigeration, showing great market potential.[7] The main raw materials for preparing LPUF are isocyanates and polyols. By adding catalysts, foaming agents, surfactants, chain extenders, and other additives, crosslinking and foaming reactions occur to form a three-dimensional network structure of the foam material. Depending on their hardness, LPUF can be classified into three categories: flexible, semi-rigid, and rigid.[8]

It is well known that fillers can improve the density and enhance the mechanical, optical, electrical, and thermal properties of polymers.[9] Therefore, efficient and economical methods for producing polymer composites without compromising their intrinsic properties have been developed. Several studies have shown that the incorporation of natural fibers into LPUF can improve the mechanical performance of the composite foams.[10,11] The addition of natural fibers endows modified LPUF with enhanced thermal stability, electrical conductivity, flame retardancy, sound absorption, and insulation properties.[12,13] Członka *et al.* investigated the effects of chemically treated eucalyptus fibers on the mechanical, thermal, and insulation properties of rigid LPUF. They treated the fibers with maleic anhydride, alkali, and silane, and reported that the silane-treated fibers exhibited significantly enhanced performance in the composite foams compared with other treatments.[14]

However, most of the raw materials currently used for synthesizing LPUF are derived from petroleum-based sources.[15] Since the 21st century, petroleum has remained one of the most dominant resources in global energy production and consumption. It is estimated that by 2050, global petroleum

[a]*State Key Laboratory of Biobased Material and Green Papermaking, Qilu University of Technology (Shandong Academy of Sciences), Jinan 250353, China. E-mail: 19854198710@163.com; wzj@qlu.edu.cn*

[b]*Shandong Yinhe Ruixue Paper Co.,Ltd, China*

[c]*Rizhao Huatai Paper Co., Ltd, Rizhao, China*

[d]*School of Environmental and Nature Resources, Zhejiang University of Science and Technology, Hangzhou 310023, China*

resources will face depletion, which will severely restrict the production and development of PU. With the depletion of petroleum resources and the increasing environmental pollution caused by petroleum-based products, researchers have turned their attention to alternative renewable resources.[16] The development and utilization of sustainable, green, and renewable materials have become a global consensus.

Kraft lignin is one of the most abundant renewable natural aromatic polymers on Earth. It is a three-dimensional network polymer composed of phenylpropane units linked by –O– and C–C bonds.[17,18] However, as a byproduct of the pulping and papermaking process, Kraft lignin is typically recovered and used as boiler fuel in pulp and paper mills, with only about 5% utilized for other purposes, leading to severe resource waste and environmental pollution.[19,20] In the preparation of LPUF, Kraft lignin can function as a polyol.[21,22] Incorporating Kraft lignin into PU production not only reduces the consumption of petroleum-based raw materials but also improves the mechanical quality of PU and introduces additional functionalities such as flame retardancy, UV resistance, and hydrophobicity.[23–25] Therefore, Kraft lignin can be incorporated into LPUF through physical blending methods.

In this study, Kraft lignin was physically blended with PEG 400 and glycerol to prepare LP, which was then combined with PMDI, water, surfactant, and catalyst for one-step foaming to synthesize LPUF. Bleached softwood pulp fibers were incorporated at varying loadings (0–1.0 wt%) as reinforcements. The resulting foams were characterized by FT-IR, NMR, SEM, optical microscopy, contact angle measurements, thermal conductivity, apparent density, and polyol property tests, along with a brief mechanical performance evaluation to assess the influence of fiber addition on the overall foam properties.

2 Materials and methods

2.1 Materials

Kraft lignin and bleached softwood kraft pulp board were supplied by Rizhao Huatai Paper Industry. PMDI, PEG-400, glycerol, silicone surfactant L580, and dibutyltin dilaurate catalyst (DBTDL) were purchased from Shanghai McLin Biochemical Technology Co., Ltd, and deionized water was prepared in-house. L580 acted as the foam stabilizer and DBTDL served as the gelation catalyst.

2.2 Preparation of lignin polyols

KL was dried at 60 °C under vacuum oven overnight and grounded to pass 80 mesh. PEG-400 and glycerol were weighed at a mass ratio of 3.5 to 0.5 and premixed at room temperature with a high-speed stirrer until homogeneous. Then KL was added to reach a total mass ratio of KL to PEG-400 to glycerol of 3 to 3.5 to 0.5. The slurry was stirred vigorously at 1000 rpm for 3 min at room temperature to obtain a uniform lignin polyol, hereafter denoted as LP.

2.3 Preparation of cellulose fiber reinforced lignin-based polyurethane foam

The pulp fiber board was cut into 2–3 cm pieces, and soaked in deionized water to swell, disintegrated to single fibers with a disintegrator, and finally air-dried to 5.8% moisture. Fibers at 0, 0.2, 0.5, 0.7 and 1.0 wt% were then blended with lignin polyol. Ten grams of lignin polyol was charged into a beaker. Then DBTDL(0.08 g), L580 (0.8 g), and water (200 μL) were added into lignin polyol. The mixture was stirred at 500 rpm for 1 min with a high-speed stirrer to give a uniform white component. Ten grams of PMDI was then added, and the blend was rapidly stirred at 3000 rpm until a milky appearance formed. Stirring was stopped and the mixture was allowed to free-rise. The total mixing time was 2–3 min. After foaming, the foam was cured in an oven at 45 °C for 24 h. The detailed formulation and process conditions are listed in Table 1. All steps were performed at ambient temperature and under normal atmospheric pressure to avoid premature reactions. The foams were trimmed after curing prior to testing.

2.4 Characterization

FT-IR was used to analyze the chemical structure of lignin and lignin polyol, with a wavenumber range of 400–4000 cm^{-1}, a resolution of 4 cm^{-1}, and 32 scans. The nuclear magnetic resonance (NMR) phosphorus spectra and 2D spectra of lignin and polyol were detected according to the referenced methods. The characterization in this study mainly includes the mechanical properties, thermal conductivity, apparent density of the foam, and related tests for lignin-based polyol. The compressive properties of the foam were measured using a texture analyzer (TA.XT Plus) according to the GB/T 8813-2020 standard, with a testing speed of 5 mm min^{-1} and compressive stress at 10% relative deformation, which is considered the compressive strength of the foam sample. The bending and tensile properties of the foam were measured using a universal testing machine (HCMMW-10L) according to the GB/T 8812-2007 standard, with a bending test speed of 20 mm min^{-1} and a tensile test speed of 10 mm min^{-1}. At least 5 samples were tested for each test. The thermal conductivity of the foam was

Table 1 Formulations of LPUF with different pulp-fiber loadings

Sample	LP (g)	DBTDL (g)	L580 (g)	Water (μL)	PMDI (g)	Fiber loading (g)
LPUF-0	10	0.08	0.8	200	10	0
LPUF-0.2	10	0.08	0.8	200	10	0.02
LPUF-0.5	10	0.08	0.8	200	10	0.05
LPUF-0.7	10	0.08	0.8	200	10	0.07
LPUF-1.0	10	0.08	0.8	200	10	0.1

measured using a thermal conductivity meter (TC3100 XIATECH, China). The apparent density of the foam was measured according to the GB/T 6343-2009 standard, and the hydroxyl value, acid value, and viscosity of lignin-based polyol were tested according to the GB/T 12008.3-2009, GB/T 12008.5-2010 and GB/T 12008.7-2010 standards, respectively. Additionally, optical microscope images of fiber slurry boards were used to observe the fiber morphology and dispersion, in order to assess their impact on the foam properties.

3 Results and discussion

3.1 Characterization of lignin and lignin polyols

The LP as a homogeneous black viscous liquid with no visible sedimentation or gelation were shown in Fig. 1. Fibers at different loadings were thoroughly mixed into the lignin polyol, and the LP indices are summarized in Table 2. As a filler, the only evident effect of fibers on LP was a pronounced increase in viscosity; as the loading increased, the viscosity rose from 2638 to 4023 mPa s. This is attributed to the hygroscopicity and swelling of the unmodified plant fibers used here, which increased the viscosity of the reaction mixture.

Fig. 2a shows the FTIR spectra of KL and LP. Both exhibit a broad O–H stretch at 3400 cm^{-1}, which is broader and more intense in LP, consistent with increased hydroxyl content introduced by PEG-400 and glycerol. The aromatic skeletal bands at 1597 (ref. 26) and 1510 cm^{-1} confirm retention of the lignin backbone. LP displays a distinct carbonyl band at 1735–1750 cm^{-1} assigned to C=O stretching, absent or weak in KL, indicating formation of carbonyl-containing species during modification. Aliphatic C–H bands at 2930 and 2850 cm^{-1} are enhanced in LP,[27] while the C–O region at 1030–1100 cm^{-1} shows redistribution from phenolic C–O toward ether C–O–C. Collectively, these features indicate a shift from phenolic-dominated KL to an aliphatic–OH– and carbonyl-rich LP, which is favorable for subsequent reactions with isocyanates.

Fig. 2b presents the 2D HSQC spectrum of KL. The aromatic region shows clear G2, G5, and G6 cross peaks that confirm guaiacyl units as the dominant motif. A sharp OMe signal is evident, indicating abundant methoxyl substitution. In the side-chain region, correlations assigned to β-O-4 linkages appear as A_α, A_β, and A_γ, together with β-5 phenylcoumaran signals B_α, B_β, and B_γ and β-β resinol signals C_α, C_β, and C_γ. These features demonstrate that KL retains the typical interunit linkages and methoxylation pattern of guaiacyl-rich lignin.

Fig. 2c and d compare the ^{31}P NMR spectra of KL and LP. In KL, Aliph-OH is 1.19 mmol g^{-1}, S–OH 1.11 mmol g^{-1}, G-OH 2.19 mmol g^{-1}, with minor H–OH 0.40 mmol g^{-1} and COOH 0.55 mmol g^{-1}. In LP, Aliph-OH increases to 5.68 mmol g^{-1}, G-OH decreases to 0.23 mmol g^{-1}, S–OH is barely visible, and COOH is not detected. These results indicate marked dilution of phenolic sites and enrichment of aliphatic hydroxyls due to PEG-400 and glycerol, giving a higher hydroxyl density dominated by Aliph-OH and greater expected reactivity toward isocyanates. FTIR corroborates this shift by showing a stronger and broader O–H band, enhanced aliphatic C–H, the appearance of a carbonyl band, and a redistribution in the C–O region from phenolic C–O toward ether C–O–C in LP.

Fig. 1 Appearance of LP.

Table 2 LP properties *vs.* fiber loading-viscosity, hydroxyl value, acid value, and moisture

Sample	Viscosity (mPa s)	Hydroxyl value (mg KOH per g)	Acid value (mg KOH per g)	Moisture (%)
LPUF-0	2638	280.5	3.927	3.687
LPUF-0.2	2851	278.6	4.023	3.564
LPUF-0.5	3164	279.2	3.956	3.861
LPUF-0.7	3675	277.3	3.859	3.634
LPUF-1.0	4023	275.5	3.762	3.701

3.2 Pulp fiber optical micrograph

The optical micrographs of bleached softwood kraft pulp fibers used as reinforcement in lignin-based polyurethane foams were shown in Fig. 3. The fibers display uniform morphology with lengths of 3–4 mm and a width near 50 μm, and they are well dispersed in the lignin polyol. This high-aspect-ratio network stabilizes cells during foaming, bridges adjacent cell walls, and suppresses crack propagation, thereby improving compressive and flexural strength. In this study the fiber dimensions were fixed while only the loading was varied, so performance changes arise from dosage effects rather than size effects. Increasing loading increases entanglement density and the number of fiber-cell contacts, though excessive contents can raise viscosity and hinder bubble growth. Overall, adjusting fiber loading offers a practical means to tune cell uniformity, mechanical robustness, and thermal insulation of the foams.

3.3 LPUF contact angle

The effect of fiber loading on the water contact angle of LPUF were shown in Fig. 4. The addition of fibers markedly alters surface wettability. At 0.5% loading the contact angle reaches 135.6°, which is 42.0° higher than LPUF-0 at 93.6°, indicating that an optimal dosage enhances hydrophobicity. The improvement likely arises from fiber-induced micro-roughness and trapped air that promote a Cassie-type wetting state. When the loading increases to 1.0% the angle drops to 87.5°, which is 6.1° lower than LPUF-0, suggesting that excessive fibers expose hydrophilic cellulose and create a more open skin, thereby reducing the apparent contact angle. Overall, fiber dosage

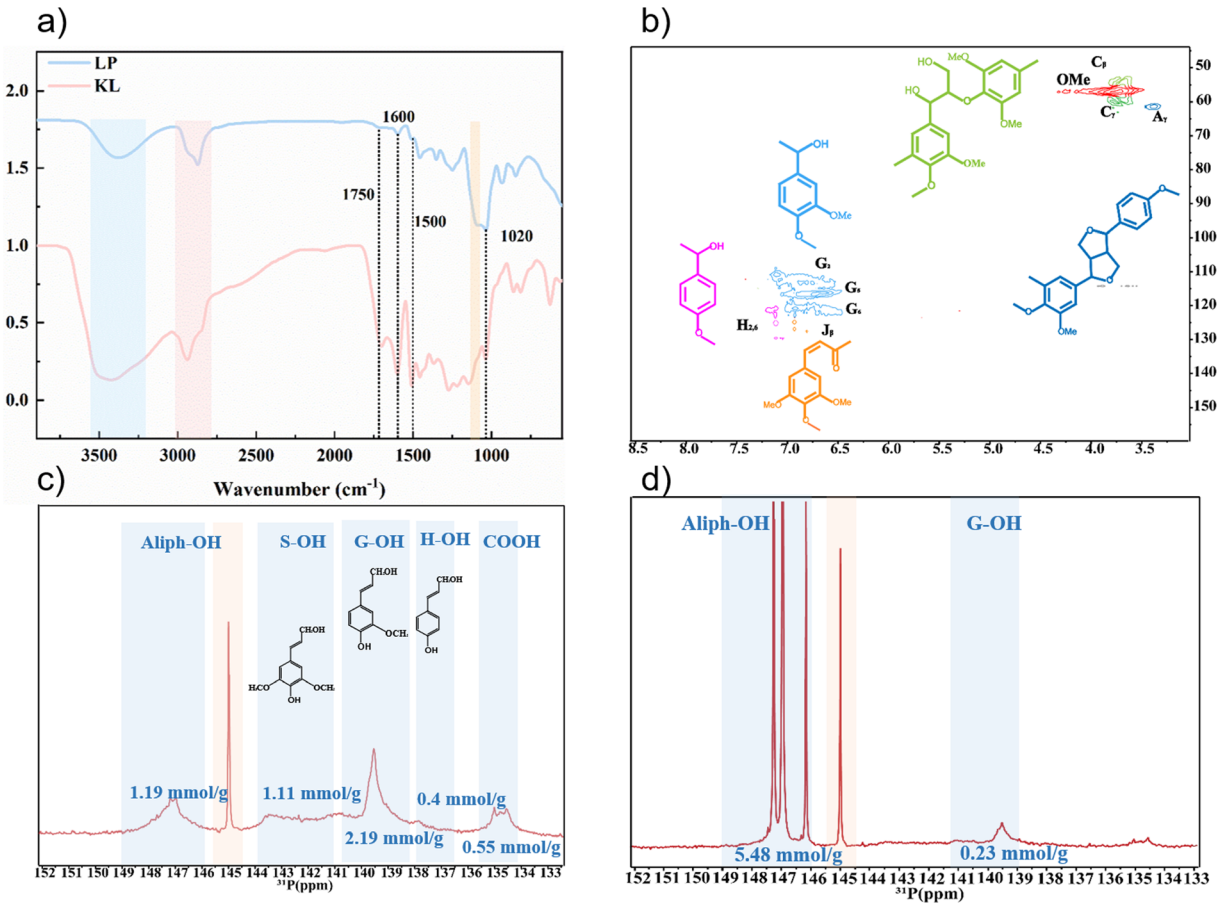

Fig. 2 (a) FTIR spectra of KL and LP; (b) 2D HSQC spectrum of KL; (c) ^{31}P NMR spectrum of LP; (d) ^{31}P NMR spectrum of KL.

Fig. 3 Macroscopic photograph of bleached softwood kraft pulp board and optical micrographs.

governs LPUF hydrophobicity, with an optimum near 0.5% and a decline at higher contents.

3.4 SEM image of LPUF

The SEM cross-sections of LPUF with increasing fiber loadings were shown in Fig. 5. Relative to LPUF-0, the addition of fibers enlarges the average cell size, broadens the size distribution, and makes the packing more irregular, with the effect pronounced at 0.7% and 1.0%. At low to moderate dosages, fibers act as heterogeneous nucleants and local reinforcements, which stabilizes incipient cells, limits early collapse, and slightly thickens struts. As loading rises, the viscosity of the reacting polyol increases and gas drainage slows, so transient cell walls resist rupture and bubbles coarsen, producing larger and less uniformly arranged cells. Occasional fiber bundles further disturb the expanding fronts and create wall defects, which contributes to cell anisotropy and uneven interconnectivity. The micrographs therefore indicate a trade-off: moderate loading stabilizes the structure and reduces collapse, whereas excessive loading introduces coarsening, irregular packing, and a higher fraction of defective walls. Controlling fiber dosage is thus an effective handle to tune cell size, wall thickness, and open-to-closed cell ratio for targeted mechanical and thermal performance.

3.5 Physical properties of LPUF

Fig. 6a shows the PUFs prepared with LP and varying pulp fiber loadings, compared to foams made with conventional petroleum-based polyol. As the lignin content increased, the foam color gradually shifted from pale yellow to dark brown. The addition of pulp fibers led to subtle fiber strands appearing on the foam surface, though there were no significant changes in the overall appearance.

Fig. 6b shows the apparent density of LPUF with different pulp fiber loadings. As fiber content increased, the density initially rose and then decreased, peaking at 108.4 kg m^{-3} at

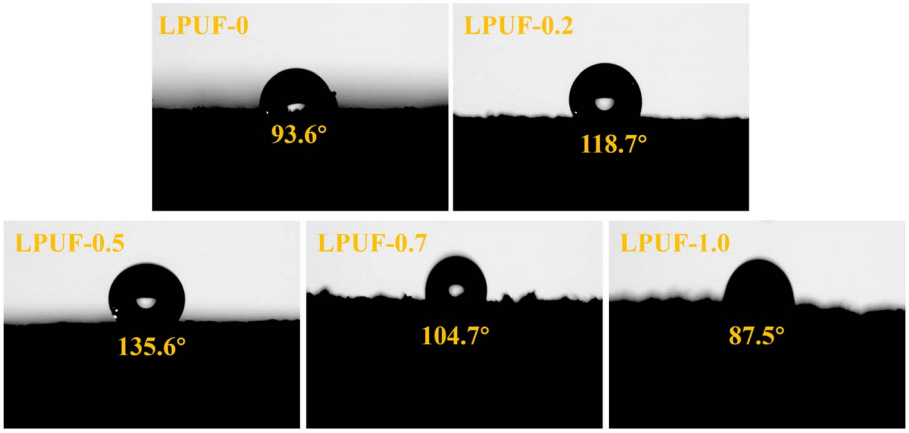

Fig. 4 Static water contact angles of LPUF at fiber loadings 0, 0.2, 0.5, 0.7, and 1.0%.

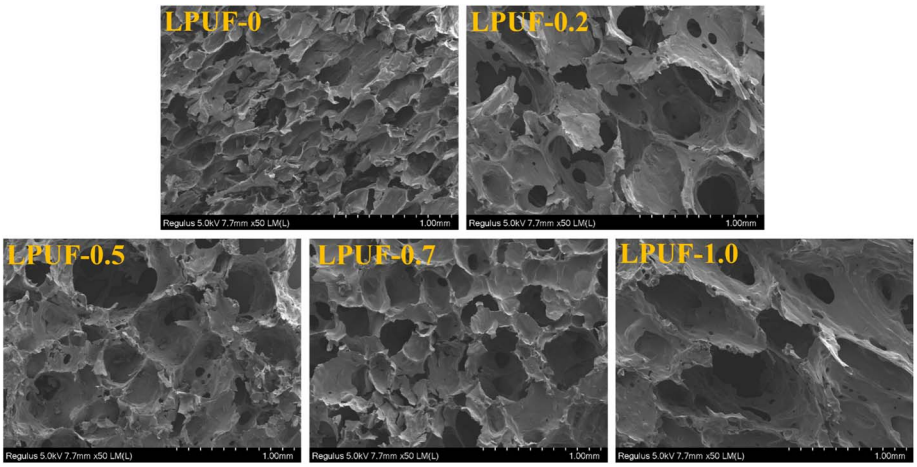

Fig. 5 SEM cross-sections of LPUF at fiber loadings 0, 0.2, 0.5, 0.7, and 1.0%.

0.5% fiber loading. Specifically, as fiber content increased from 0% to 0.5%, the density increased from 94.75 kg m^{-3} to 108.4 kg m^{-3}, likely due to fibers filling voids in the lignin polyol matrix. However, as the fiber content reached 1.0%, the density decreased to 99.6 kg m^{-3}, indicating that excessive fiber loading can distort pore morphology, making pore size larger and arrangement more irregular, which reduces the foam's density. This is supported by the SEM results, suggesting that high fiber content negatively impacts the foam's microstructure and compactness.

Fig. 6c shows the effect of fiber loading on the thermal conductivity of LPUF. Compared to LPUF-0, the addition of fibers effectively reduced thermal conductivity. At 0.5% fiber loading, the thermal conductivity of LPUF-0.5 decreased to 0.0378 W m^{-1} K^{-1}, falling within the range typically required for insulation materials (0.02 W m^{-1} K^{-1} to 0.04 W m^{-1} K^{-1}). A more uniform and complete pore structure helps reduce the thermal conduction path, thereby lowering thermal conductivity, which is consistent with the SEM results. However, when the fiber loading increased to 1.0%, the thermal conductivity slightly increased, likely due to excessive fiber content causing irregular pore morphology, larger pore size, and an increased thermal conduction path.[28]

Fig. 6d shows the effect of different fiber loadings on the bending strength of LPUF. As the fiber content increased, the bending strength of LPUF initially increased and then decreased. At 0.5% fiber loading, the bending strength of LPUF-0.5 reached a maximum value of 1.28 MPa, which is a 154.5% increase compared to LPUF-0 (0.50 MPa), indicating a significant improvement. This enhancement is likely due to fibers acting as a "reinforced skeleton", improving the foam structure and mechanical properties. However, further increasing the fiber loading led to a decrease in bending strength, possibly because of phase separation between the hydrophobic polyurethane matrix and hydrophilic fibers, which results in structural instability. The fibers absorb water and clump together, creating voids. As fiber content increases, this separation becomes more pronounced, limiting stress transfer and decreasing bending strength. This phenomenon is consistent with previous studies on fiber dispersion and structural uniformity. In conclusion, an optimal fiber content, particularly 0.5%, significantly enhances bending strength, while excessive

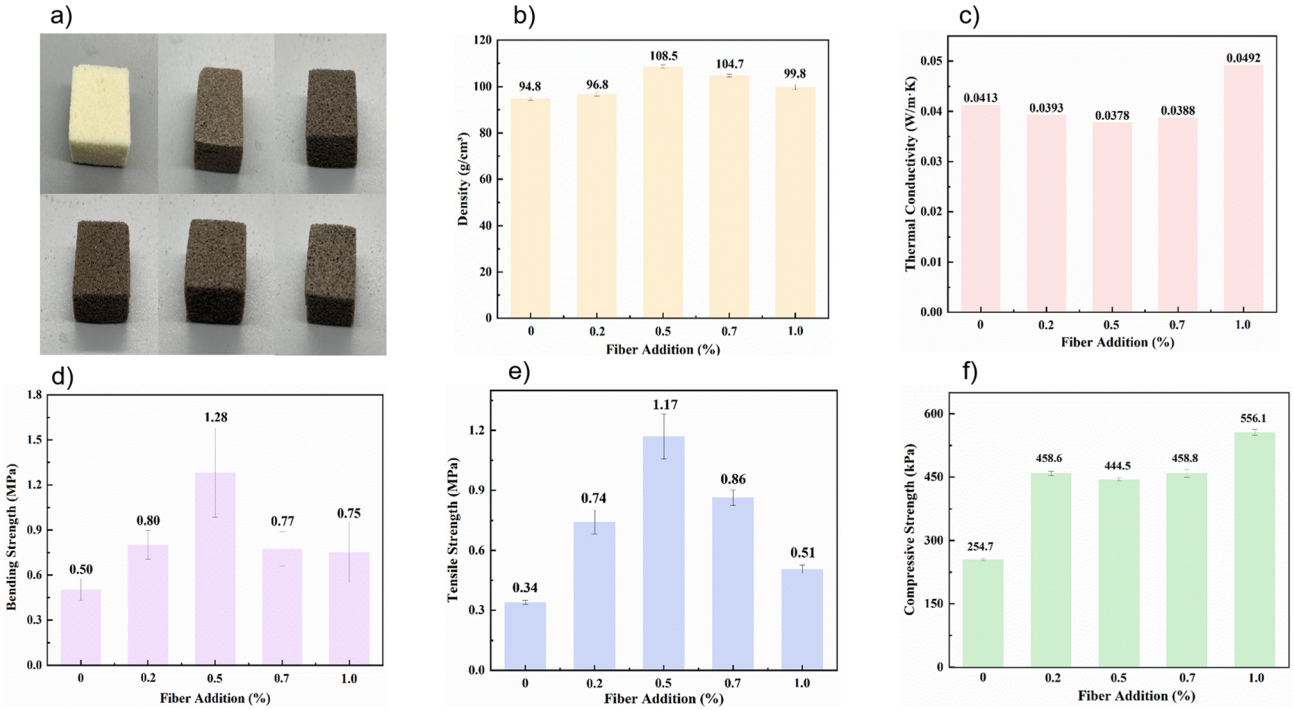

Fig. 6 (a) Photographs of LPUF with different fiber loadings; (b) apparent density; (c) thermal conductivity; (d) bending strength; (e) tensile strength; (f) compressive strength at 10% strain.

fiber content, especially at 1.0%, leads to an uneven foam structure and decreased performance.

Fig. 6e shows the effect of different fiber loadings on the tensile strength of LPUF. The addition of fibers significantly improved the tensile strength of LPUF. At 0.5% fiber loading, the tensile strength reached its maximum value of 1.17 MPa, a 244.1% increase compared to LPUF without fibers, which had a tensile strength of 0.34 MPa. This increase is likely due to fibers partially inhibiting the foaming reaction, reducing the reaction rate, and promoting greater crosslinking in LPUF, making the foam structure more robust and capable of withstanding tensile stress. However, when the fiber loading increased to 1.0%, the tensile strength decreased to 0.51 MPa. This decline may be attributed to excessive fiber content causing an uneven internal foam structure, where fiber aggregation leads to irregular pore formation that compromises tensile performance. Therefore, carefully controlling fiber content is essential for optimizing the foam's tensile properties.

Fig. 6f shows the compressive strength of LPUF at 10% strain as a function of fiber loading. Strength increases with fiber content and reaches 556.1 kPa at 1.0%, which is 118.3% higher than LPUF-0 at 254.7 kPa, indicating effective reinforcement by the fibers. The trend is not strictly monotonic: intermediate loadings give 488.6 kPa at 0.2%, 444.5 kPa at 0.5%, and 458.8 kPa at 0.7%, reflecting the balance between cell-wall stabilization by fibers and viscosity-induced coarsening. Additional measurements at 30% strain show a maximum for LPUF-0.5 at 647.6 kPa, a 72.3% increase over LPUF-0 at 375.8 kPa, which suggests that moderate loading better preserves the load-bearing architecture at higher strain. At excessive loadings, limited interfacial bonding and hindered expansion increase density yet introduce irregular cells, offsetting the reinforcement and reducing compressive performance, in agreement with SEM observations. Through a review of the literature, it can be seen that our study demonstrates significant advantages in physical properties compared with other polyurethane foams.[29,30]

3.6 Innovation points

The creativity of this work lies in the simple and solvent-free preparation of lignin-based polyol by directly blending Kraft lignin with PEG and glycerol, followed by one-step foaming to produce LPUF. In addition, a very low loading of untreated cellulose fibers (only 0.5%) is sufficient to simultaneously enhance mechanical properties and reduce thermal conductivity, without chemical modification of either lignin or fibers. Compared with previously reported lignin- or fiber-reinforced polyurethane foams, this approach offers a facile, low-cost, and scalable route, while achieving competitive mechanical strength and thermal insulation performance. These aspects have been further emphasized in the revised manuscript to clearly highlight the novelty and practical significance of this study.

4 Conclusion

This study demonstrates that fiber loading significantly influences the performance of LPUF. At a 0.5% fiber loading, bending strength increased by 154.5%, tensile strength by 244.1%, and thermal conductivity decreased to 0.0378 W m^{-1}

K^{-1}, all within the ideal range. The 0.5% fiber loading not only optimized the foam's mechanical properties but also effectively reduced thermal conductivity, highlighting its potential for thermal insulation applications. However, excessive fiber content, particularly at 1.0%, results in an uneven microstructure, with compressive strength and tensile strength decreasing to 556.1 kPa and 0.51 MPa, respectively. This suggests that excessive fiber negatively impacts foam performance. Thus, an optimal fiber content, especially around 0.5%, offers the best balance for LPUF performance. Future research should focus on improving fiber dispersion and enhancing interactions with lignin-based polyol, while exploring practical applications in construction, insulation materials, and sustainable packaging.

Conflicts of interest

There are no conflicts to declare.

Data availability

All the data supporting the results of this study can be found in this article.

Acknowledgements

The work was supported by Shandong Technological Innovation Guidance Program (Project No. YDZX2024140), and Shandong Key Research and Development Program (Project No. 2025CXGC011002).

References

1 N. V. Gama, A. Ferreira and A. Barros-Timmons, Polyurethane Foams: Past, Present, and Future, *Materials*, 2018, **11**(10), 1841.
2 A. Kemona and M. Piotrowska, Polyurethane Recycling and Disposal: Methods and Prospects, *Polymers*, 2020, **12**(8), 1752.
3 F. M. de Souza, P. K. Kahol, and R. K. Gupta, Introduction to Polyurethane Chemistry, in *Polyurethane Chemistry: Renewable Polyols and Isocyanates*, American Chemical Society, 2021, vol. 1380, pp. 1–24.
4 F. M. de Souza, M. R. Sulaiman, and R. K. Gupta, Materials and Chemistry of Polyurethanes, in *Materials and Chemistry of Flame-Retardant Polyurethanes Volume 1: A Fundamental Approach*, American Chemical Society, 2021, vol. 1399, pp. 1–36.
5 A. M. Borrero-López, V. Nicolas, Z. Marie, A. Celzard and V. Fierro, A Review of Rigid Polymeric Cellular Foams and Their Greener Tannin-Based Alternatives, *Polymers*, 2022, **14**(19), 3974.
6 J. Wang, C. Zhang, Y. Deng and P. Zhang, A Review of Research on the Effect of Temperature on the Properties of Polyurethane Foams, *Polymers*, 2022, 4586.
7 V. Yakushin, V. Dhalivala, L. Vevere and U. Cabulis, Influence of Rigid Polyurethane Foam Production Technology on Cryogenic Water Uptake, *Polymers*, 2025, 1669.
8 A. A. Maamoun, M. Arafa and A. M. K. Esawi, Flexible polyurethane foam: materials, synthesis, recycling, and applications in energy harvesting – a review, *Mater. Adv.*, 2025, **6**(6), 1842–1858.
9 S. C. Daminabo, S. Goel, S. A. Grammatikos, H. Y. Nezhad and V. K. Thakur, Fused deposition modeling-based additive manufacturing (3D printing): techniques for polymer material systems, *Mater. Today Chem.*, 2020, **16**, 100248.
10 C. Kuranchie, A. Yaya and Y. D. Bensah, The effect of natural fibre reinforcement on polyurethane composite foams – A review, *Sci. Afr.*, 2021, **11**, e00722.
11 G. E. Pech-Can, E. A. Flores-Johnson, J. G. Carrillo, E. Bele and A. Valadez-Gonzalez, Mechanical Properties of Polyurethane Foam Reinforced with Natural Henequen Fibre, *J. Compos. Sci.*, 2024, **8**(9), 343.
12 H. Dong, S. Li, Z. Jia, Y. Luo, Y. Chen, J. Jiang and S. Ji, A Review of Polyurethane Foams for Multi-Functional and High-Performance Applications, *Polymers*, 2024, 3182.
13 B. Masruri, E. Taban, A. Khavanin and K. Attenborough, Sound Absorption and Thermal Insulation by Polyurethane Foams Reinforced with Bio-Based Lignocellulosic Fillers: Data and Modeling, *Buildings*, 2025, **15**(19), 3590.
14 S. Członka, A. Strąkowska, P. Pospiech and K. Strzelec, Effects of Chemically Treated Eucalyptus Fibers on Mechanical, Thermal and Insulating Properties of Polyurethane Composite Foams, *Materials*, 2020, **13**(7), 1781.
15 M. Santos, M. Mariz, I. Tiago, S. Alarico and P. Ferreira, Bio-Based Polyurethane Foams: Feedstocks, Synthesis, and Applications, *Biomolecules*, 2025, **15**(5), 680.
16 T. A. Phung Hai, M. Tessman, N. Neelakantan, A. A. Samoylov, Y. Ito, B. S. Rajput, N. Pourahmady and M. D. Burkart, Renewable Polyurethanes from Sustainable Biological Precursors, *Biomacromolecules*, 2021, **22**(5), 1770–1794.
17 R. Nadányi, A. Ház, A. Lisý, M. Jablonský, I. Šurina, V. Majová and A. Baco, Lignin Modifications, Applications, and Possible Market Prices, *Energies*, 2022, **15**(18), 6520.
18 S. E. Klein, J. Rumpf, P. Kusch, R. Albach, M. Rehahn, S. Witzleben and M. Schulze, Unmodified kraft lignin isolated at room temperature from aqueous solution for preparation of highly flexible transparent polyurethane coatings, *RSC Adv.*, 2018, **8**(71), 40765–40777.
19 C. Huang, Z. Peng, J. Li, X. Li, X. Jiang and Y. Dong, Unlocking the role of lignin for preparing the lignin-based wood adhesive: A review, *Ind. Crops Prod.*, 2022, **187**, 115388.
20 R. S. Abolore, S. Jaiswal and A. K. Jaiswal, A comprehensive review on sustainable lignin extraction techniques, modifications, and emerging applications, *Ind. Crops Prod.*, 2025, **235**, 121696.
21 F. R. Vieira, N. V. Gama, D. V. Evtuguin, C. O. Amorim, V. S. Amaral, P. C. O. R. Pinto and A. Barros-Timmons, Bio-Based Polyurethane Foams from Kraft Lignin with Improved Fire Resistance, *Polymers*, 2023, **15**(5), 1074.

22 C. S. Carriço, T. Fraga and V. M. D. Pasa, Production and characterization of polyurethane foams from a simple mixture of castor oil, crude glycerol and untreated lignin as bio-based polyols, *Eur. Polym. J.*, 2016, **85**, 53–61.
23 T. Xiao, L. Wu, Q. Xu, X. Yu, Q. Fu, F. Zhang, Y. Li, G. Yin, L. Huang, P. Fatehi and H. Shi, Highly-Flame-Retardant Performance and Sustainable Polyurethane Foams from Industrial Kraft Lignin *via* Exploiting Lignin Demethylation, *Biomacromolecules*, 2025, **26**(10), 6444–6457.
24 J. Hu, M. Huang, X. Zhou, R. Luo, L. Li and X. Li, Research Status of Lignin-Based Polyurethane and Its Application in Flexible Electronics, *Polymers*, 2024, **16**(16), 2340.
25 A. Shafiq, I. Ahmad Bhatti, N. Amjed, M. Zeshan, A. Zaheer, A. Kamal, S. Naz and T. Rasheed, Lignin derived polyurethanes: Current advances and future prospects in synthesis and applications, *Eur. Polym. J.*, 2024, **209**, 112899.
26 W. Zhang, Y. F. Ma, C. P. Wang, S. H. Li, M. M. Zhang and F. X. Chu, Preparation and properties of lignin-phenol-formaldehyde resins based on different biorefinery residues of agricultural biomass, *Ind. Crops Prod.*, 2013, **43**, 326–333.
27 M. N. A. Yaakob, R. Roslan, N. Salim, and S. N. H. Mustapha, in *Structural and Thermal Behavior of Lignin-Based Formaldehyde-free Phenolic Resin*, 3rd Symposium on Industrial Science and Technology (SISTEC), Kuantan, MALAYSIA, Aug 25-26; Kuantan, MALAYSIA, 2021, pp. 1388–1391.
28 K. Fu, L. Zhang, Y. Lin, W. Zhang, Z. Zhao, W. Chen and C. Chang, Valorization of xylose residues and crude glycerol for production of biopolyurethane foam, *Waste Biomass Valoriz.*, 2024, 1–15.
29 J. Wang, C. X. Zhang, Y. Deng and P. Zhang, A Review of Research on the Effect of Temperature on the Properties of Polyurethane Foams, *Polymers*, 2022, **14**(21), 4586.
30 Y. Li, Y. M. Han, T. F. Qin and F. X. Chu, Preparation of Polyurethane Foams Based on Liquefied Corn Stalk Enzymatic Hydrolysis Lignin, *J. Biobased Mater. Bioenergy*, 2012, **6**(1), 51–58.